

Original Research

# Functional and Mechanistic Insights into the Fatty-Acid CoA Ligase FadK in *Escherichia coli*

Dafeng Liu<sup>1,2,\*</sup>, Ablikim Abdiriyim<sup>1</sup>, Lvxia Zhang<sup>1</sup>, Feng Yu<sup>1</sup>

Academic Editor: Catarina M. Paquete

Submitted: 2 January 2025 Revised: 6 March 2025 Accepted: 12 March 2025 Published: 24 April 2025

#### **Abstract**

**Background**: *Escherichia coli* (*E. coli*) is a common opportunistic bacterial pathogen in both human and animal populations. Fatty acids serve as the central carbon and energy source, a process mediated by fatty acid-coenzyme A (CoA) ligases encoded by *fad* genes such as *FadK*. However, the function and the mechanism of FadK remain unclear. **Methods**: The three-dimensional structure of FadK was modeled using AlphaFold2. After expression and purification, monomeric FadK was successfully isolated. The enzymatic activity was assayed, and real-time quantitative polymerase chain reaction (RT-qPCR) was performed to quantify *FadK* expression levels. **Results**: In enzymatic assays of fatty acid CoA ligase activity, caprylic acid was found to be the optimal substrate for FadK. We determined the optimal catalytic conditions for FadK, which include a pH of 7.4, ATP concentration of 0.6 mM, CoA concentration of 0.8 mM, and Mg<sup>2+</sup> concentration of 0.8 mM at 37 °C. Notably, the activity of FadK showed a decrease with increasing concentrations of dodecyl-AMP, which was further confirmed by the RT-qPCR results. **Conclusions**: Our findings will serve as a fundamental framework for the development of innovative therapeutics that target *E. coli* infections.

Keywords: Escherichia coli; fatty-acid CoA ligase FadK; enzyme activity; gene expression levels; inhibitor dodecyl-AMP

#### 1. Introduction

Escherichia coli (E. coli) is the predominant opportunistic bacterial pathogen affecting both human and animal populations [1,2]. This microorganism is responsible for a wide range of nosocomial and community-acquired diseases, particularly gastroenteritis, urinary tract infections, and bacteremia [3,4]. Despite varying susceptibility profiles to conventional therapeutic antimicrobials, E. coli has the potential to acquire resistance determinants via horizontal gene transfer, both within and between species, accelerating the proliferation of drug-resistant bacterial strains [5–7]. Of great concern is the emergence of multidrug-resistant E. coli, which represents a major public health challenge due to the decreasing efficacy of existing antibiotic therapies [3,4,8–10]. Therefore, it is urgent to take immediate measures to control or even end the situations.

Bacterial species possess a diverse and distinct array of lipids, which play a critical role in their pathogenic mechanisms and disease development [11–17]. These microorganisms encounter numerous environmental stressors, including fluctuations in pH, reactive oxygen species, enzymatic breakdown, and shortages of vital nutrients or nitrogen compounds [16–21]. Such hostile conditions frequently compromise the integrity of their lipid-dense cellular membranes, which are targeted by host defense systems [14,20–22]. To ensure survival, bacteria have developed sophisticated mechanisms to adapt their lipid-dense cellular membranes. These structures are produced through the ac-

tivity of key enzymes such as fatty acid-coenzyme A (CoA) ligases and acyl-CoA synthetases [12,16,17,20,21,23–28], which are important targets for developing new antibacterial drugs. In *E. coli*, the fatty acid-CoA ligase FadK exhibits substrate specificity for short-chain fatty acids (below C<sub>10</sub>) and contributes to their anaerobic metabolic processing [29]. *E. coli* FadK features two conserved domains: AMP-dependent synthetase domain (aa 49–415) and AMP-binding domain (aa 466–543) (Fig. 1a,b). The catalytic mechanism of FadK proceeds through a two-step reaction characterized by the formation of an acyl adenylate (acyl-AMP) intermediate (Fig. 1c). However, the function and the mechanism of *E. coli* FadK are still unknown.

Herein, we successfully obtained monomeric FadK. We identified caprylic acid as the preferred substrate for FadK in fatty acid CoA ligase activity. The optimal conditions for the catalytic reaction were found to be pH 7.4, 0.6 mM ATP, 0.8 mM CoA, 0.8 mM Mg<sup>2+</sup> at 37 °C. The enzymatic activity of FadK showed a decreasing trend with increasing concentrations of dodecyl-AMP. These findings offer substantial potential for designing innovative therapeutics targeting *E. coli* infections.

# 2. Materials and Methods

### 2.1 Protein Constructs, Expression and Purification

The primers specific to the recombinant FadK were custom-designed for PCR amplification and then synthesized by Shanghai Sangon Biotechnology (Shang-

<sup>&</sup>lt;sup>1</sup> Xinjiang Key Laboratory of Lavender Conservation and Utilization, College of Biological Sciences and Technology, Yili Normal University, 835000 Yining, Xinjiang, China

<sup>&</sup>lt;sup>2</sup>School of Life Sciences, Xiamen University, 361102 Xiamen, Fujian, China

<sup>\*</sup>Correspondence: dafeli@sina.cn (Dafeng Liu)

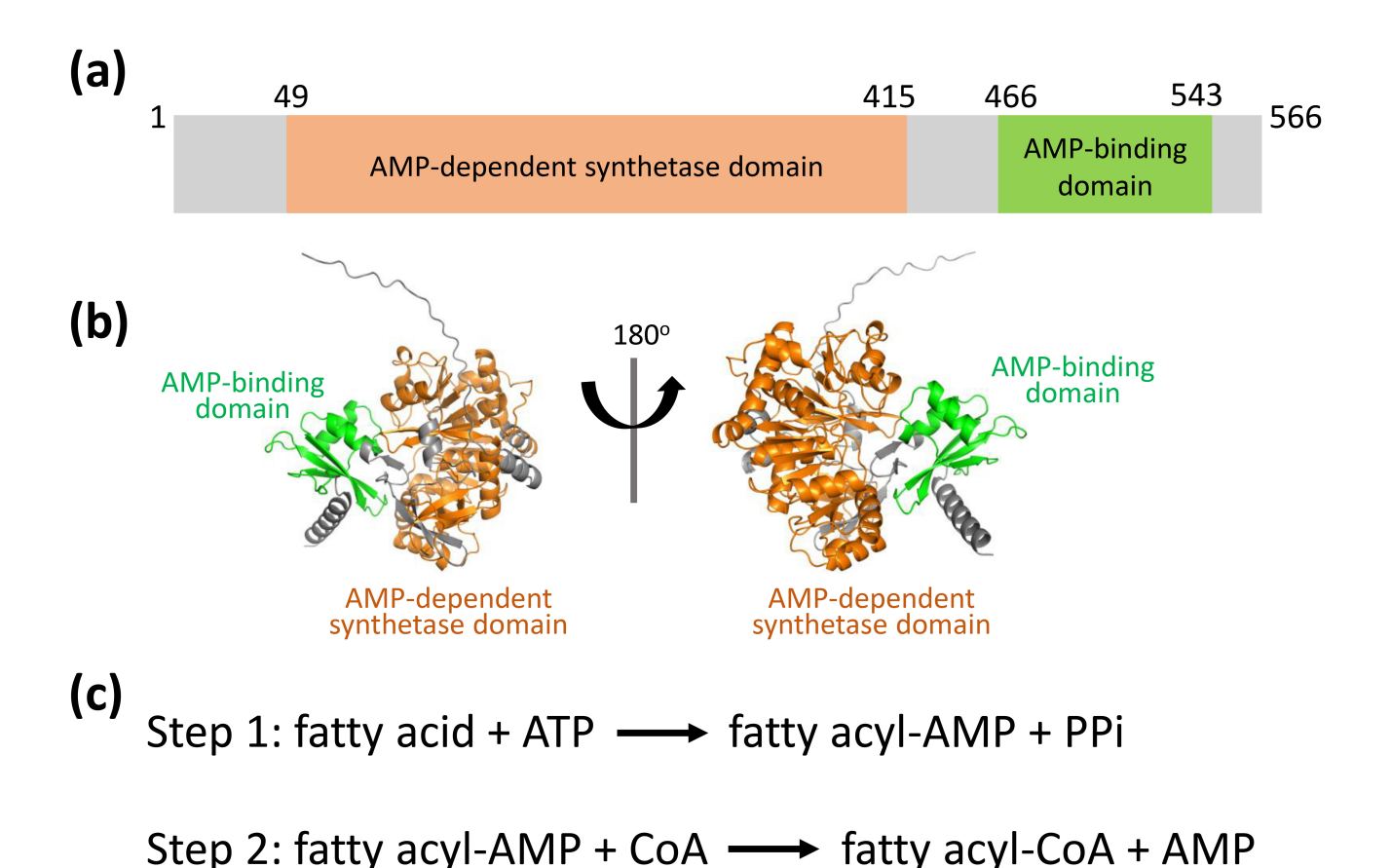


**Fig. 1. FadK structure predicted using AlphaFold2.** (a) Schematic representation of the AMP-dependent synthetase domain (aa 49–415, in orange) and the AMP-binding domain (aa 466–543, in green). (b) FadK structure predicted by AlphaFold2, ribboned, in two orientations, with the two conserved domains colored as shown in Fig. 1a. (c) The enzyme mechanism is elucidated, involving a two-step reaction marked by the generation of a fatty acyl-AMP intermediate. CoA, coenzyme A; PPi, pyrophosphoric acid.

hai, China). Subsequently, target genes were integrated into pET-28a(+) vector (Novopro, Shanghai, China) (**Supplementary Table 1**). PCR experiments were conducted utilizing Q5 polymerase (New England Biolabs, Ipswich, MA, USA). DNA sequence analysis was performed to confirm the correctness of the cloning process. The resulting plasmid constructs were then introduced into *E. coli* BL21(DE3) cells.

FadK expression on a large scale was conducted by inoculating bacterial cells (20 mL) into LB medium supplemented (1 L) with kanamycin at 45  $\mu$ g/mL, followed by overnight incubation at 37 °C. Bacterial cultures were incubated at 37 °C under constant agitation (220 rpm) until achieving an optical density (OD) of 0.6–0.8 at 600 nm. Subsequently, the culture was incubated at 25 °C with 1 mM Isopropyl  $\beta$ -D-1-thiogalactopyranoside (IPTG) for approximately 12 h to induce expression of the target protein.

Nickel-Nitrilotriacetic acid (Ni-NTA) was employed to purify various protein expression constructs of FadK according to our previous reports [30]. Bacterial cells were suspended in a buffer (150 mM NaCl, 20 mM Tris-HCl, pH 7.4, 5 mM DTT, 5% glycerol) and lysed at 650 MPa for 3 min. After centrifugation, insoluble debris was removed and the soluble lysate was applied to a Ni-NTA affinity col-

umn pre-equilibrated with the same buffer. The column was washed with appropriate buffers to remove unbound proteins. FadK was eluted with 300 mM imidazole, concentrated and further purified by size exclusion chromatography on a Superdex 200 10/300 GL column (GE Healthcare, Chicago, WI, USA).

# 2.2 Enzyme Activity Assays of FadK

FadK enzymatic activity was assessed through spectrophotometric measurement of coenzyme A (CoA) thiol group consumption, with 5,5'-dithiobis-(2-nitrobenzoic acid) (DTNB) (Sigma-Aldrich, St. Louis, MO, USA) serving as the detection reagent. This approach, adapted from established protocols [31–33], was based on the fatty-acyl-CoA ligation reaction. The interaction between free thiols and DTNB produced a chromogenic response, which was measured by absorbance at 412 nm (OD<sub>412 nm</sub>).

The enzymatic activity assay was conducted using a 90  $\mu$ L reaction solution comprising 6  $\mu$ g FadK, 10 mM ATP, varying fatty acid concentrations, 0.1 mM Tris-HCl (pH 8.0), 10 mM K<sup>+</sup> and 10 mM MgCl<sub>2</sub>. To enhance fatty acid solubility, 0.001% (w/v) Plysurf A-210G was incorporated as a dispersant. For fatty-acyl-CoA ligation activity determination, the inhibitor dodecyl-AMP was included.



After adding 10  $\mu$ L of 5 mM CoA, the mixtures were incubated at 37 °C for 2 min, allowed to rest for 5 min, and heatinactivated at 85 °C for 5 min. Post-cooling to ambient temperature, 70  $\mu$ L of the reaction sample was mixed with 600  $\mu$ L of 400  $\mu$ M DTNB in potassium phosphate buffer (pH 7.0), and absorbance at 412 nm (OD<sub>412 nm</sub>) was recorded. The DTNB extinction coefficient (13,600 M<sup>-1</sup>·cm<sup>-1</sup>) was applied to calculate specific activity. Substrate kinetics were evaluated over concentrations with Hanes-Woolf plots to determine Michaelis constant ( $K_m$ ) and catalytic activities ( $K_{cat}$ ) (Supplementary Table 2).

Control reaction mixtures in which no protein was present were included for comparison. The results were evaluated at different concentrations of substrates, Adenosine triphosphate (ATP), CoA, and magnesium ion (Mg<sup>2+</sup>) concentrations, as well as different temperatures and pH values. Additionally, the inhibitor dodecyl-AMP was introduced to the bacterial suspension.

#### 2.3 Antibacterial Activity Test

Bacterial cultures in the logarithmic growth phase were employed. Overnight cultures were adjusted to inoculum densities of  $1.73\times10^7$  CFU/mL in LB medium. Bacterial suspensions were treated with the inhibitor dodecyl-AMP at pH 7.2. Aliquots (100  $\mu L)$  of inoculum (10 $^6$  CFU/mL) were mixed with serially diluted inhibitor concentrations (two-fold dilutions) in centrifuge tubes and incubated with shaking at 37  $^{\circ}$ C for 20 h. Survival rates (%) were derived by normalizing the colony counts of inhibitor-exposed samples against untreated controls.

### 2.4 Expression Analysis of FadK Gene Using RT-qPCR

Real-time quantitative polymerase chain reaction (RTqPCR) was used to measure FadK gene expression in bacterial cultures harvested at late logarithmic growth. Cultures were exposed to dodecyl-AMP at concentrations of 2.5, 5 or 10 µM for 1 or 6 h, with the inhibitor administered as a single or split dose. Total RNA was isolated with the TransZol RNA extraction kit (Invitrogen, Carlsbad, CA, USA) according to the manufacturer's instructions. Next, cDNA was generated from the purified RNA using the PrimeScript 1st Strand cDNA Synthesis Kit (Takara, Kyoto, Japan). RTqPCR was performed with PowerUp SYBR Green Master Mix (Thermo Fisher Scientific, Waltham, MA, USA) and primers detailed in Supplementary Table 3. Amplification and quantification were carried out on an Applied Biosystems QuantStudio 5 system (Thermo Fisher Scientific, Waltham, MA, USA). Gene expression levels were analyzed via  $2^{-\Delta\Delta CT}$  method [30,34–38]. with results displayed as log2-transformed values in histograms. Ratios exceeding zero denoted up-regulated expression, whereas values below zero indicated down-regulation. The housekeeping gene gyr A [39-42] served as the reference for normalization, and its inclusion as a positive control confirmed assay validity.

#### 2.5 Statistical Analysis

All experiments were performed at least in triplicate, with results presented as means  $\pm$  standard deviation (SD). Statistical analyses were carried out using GraphPad Prism 8.0 (GraphPad Software, San Diego, CA, USA), Microsoft Excel 2013 (Microsoft Corporation, Redmond, WA, USA), and SPSS 19.0 (IBM Corp., Chicago, IL, USA). For analyses, p < 0.05 and p < 0.01 were defined as thresholds for statistical significance and high statistical significance, respectively.

# 3. Results

# 3.1 Expression and Purification of Recombinant FadK Protein

We designed and constructed prokaryotic expression plasmids to facilitate the expression of recombinant FadK protein, employing designated primers and restriction endonucleases (**Supplementary Table 1**). The induction of FadK protein expression was orchestrated within *E. coli* host cells. Subsequently, the supernatant was subjected to purification via Ni-NTA agarose affinity chromatography following cell lysis and centrifugation. To obtain highly pure FadK, purification parameters were systematically optimized. A buffer containing 150 mM NaCl, 5 mM DTT, 5% glycerol and 20 mM Tris-HCl (pH 7.4) was found to be critical to minimize non-specific hydrophobic and ionic interactions between FadK and co-purifying contaminants during chromatography. Additionally, 300 mM imidazole was added for FadK elution.

Furthermore, FadK purification was refined using the ÄKTA purification system. We found that the retention volume was 15.2 mL (Fig. 2a), implying the presence of monomeric forms of FadK protein.

Protein was collected based on the single peak observed in gel filtration chromatography. Subsequently, the protein was analyzed using 12% sodium dodecyl sulfate-polyacrylamide gel electrophoresis (SDS-PAGE), showing a band (Fig. 2b). Therefore, the high purity FadK was obtained and then used in the following experiments.

# 3.2 Caprylic Acid is the Optimal Substrate for FadK Activity

To assess the catalytic activity of FadK, we monitored the depletion of free thiol groups in CoA during FadK-catalyzed fatty acid-CoA ligation reactions [32,33,43–45]. We observed that specific activities of FadK at 253.1, 158.3, 110.6, and 98.7 nmol/min/mg protein, respectively, when utilizing caprylic acid, hexanoic acid, butyric acid, and capric acid as substrates (Fig. 3, **Supplementary Fig. 1**). In contrast, specific activities ranged from 6.4 to 39.8 nmol/min/mg protein when employing other fatty acids as substrates (Fig. 3). These showed the significantly enhanced catalytic efficiency of FadK with caprylic acid, hexanoic acid, butyric acid, and capric acid substrates compared to alternative fatty acids. Notably, FadK exhibited its utmost catalytic proficiency with caprylic acid, indicat-



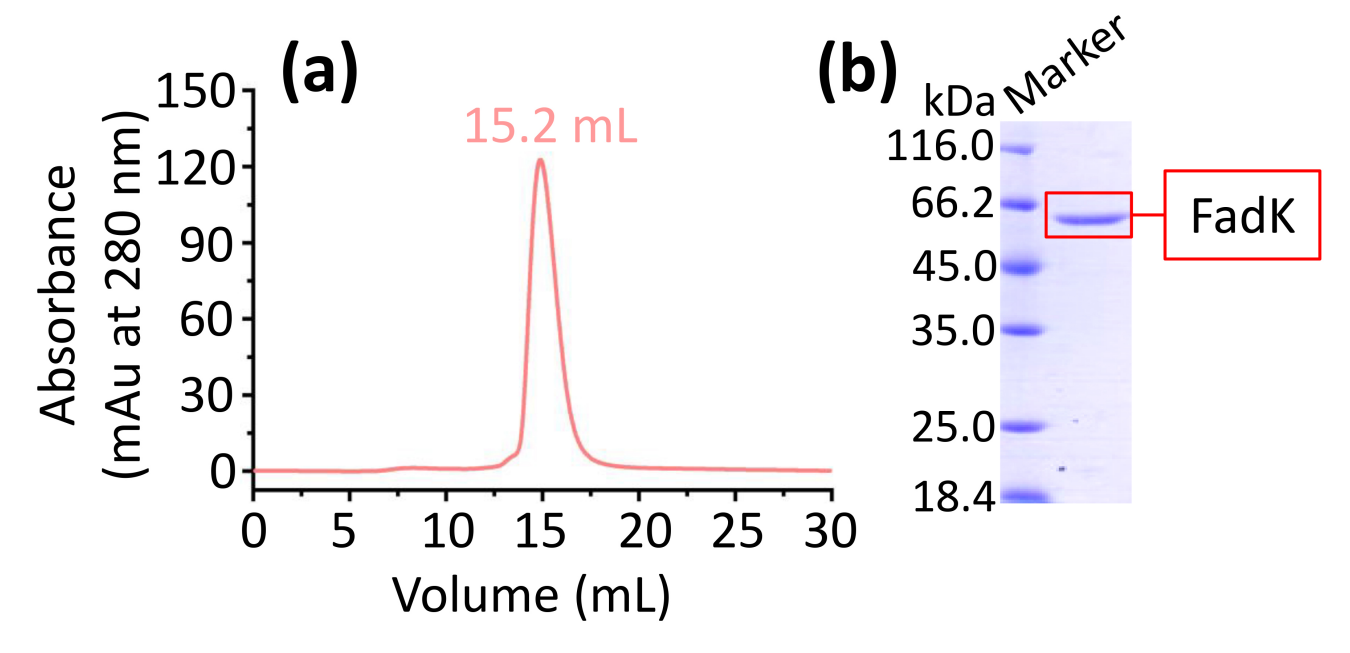


**Fig. 2.** The expression and purification of FadK. (a) FadK was purified by size-exclusion chromatography on a Superdex 200 10/300. A single peak at 15.2 mL confirmed the monomeric state of FadK. (b) The peak fraction isolated from the ÄKTA purifier-based gel filtration was further analyzed by sodium dodecyl sulfate-polyacrylamide gel electrophoresis (SDS-PAGE) via a 12% gel.

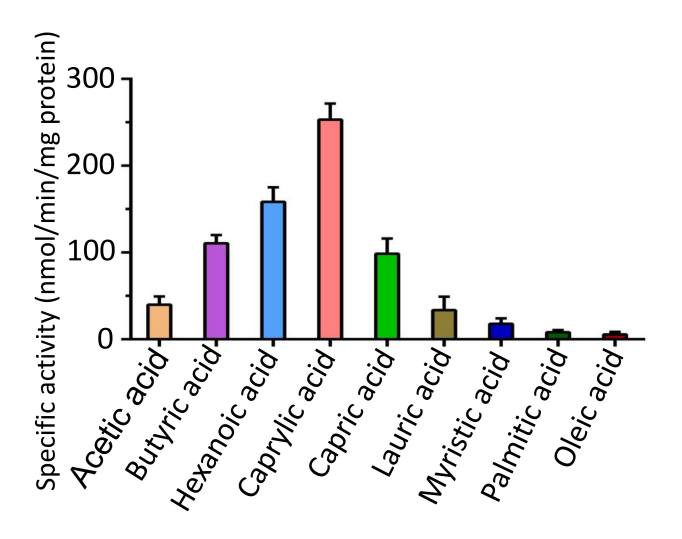


**Fig. 3. FadK different substrate specificity.** Enhanced enzymatic activities were observed with caprylic acid, hexanoic acid, butyric acid, and capric acid substrates in comparison to other fatty-acid substrates. Caprylic acid was identified as the preferred substrate for FadK among these substrates.

ing that caprylic acid is the most stable of these fatty acid substrates (Fig. 3).

The enhanced catalytic efficiency of FadK observed with caprylic acid as substrate is likely due to several factors, such as the participation of ATP and/or CoA in the catalytic process and the three-dimensional structural arrangement of the enzyme.

# 3.3 Effects of pH, ATP, CoA and $Mg^{2+}$ on the Fatty-Acid CoA Ligase Activity of FadK

To explore the optimal parameters of the fatty-acid CoA ligase activity of FadK, we focused our investigation on the catalytic properties of the substrate caprylic acid, since it's the optimal substrate for FadK (Fig. 3). We found that the fatty-acid CoA ligase activity of FadK exhibited an incremental trend with increasing pH, peaking at pH 7.4 before declining (Fig. 4a). Additionally, we observed a proportional increase in activity with increasing concentrations of ATP, reaching a peak at 0.6 mM ATP, beyond which no further increase was observed (Fig. 4b). Similarly, elevations in CoA concentration resulted in augmented activity, culminating at 0.8 mM CoA, with subsequent concentrations eliciting no additional effect (Fig. 4c). Furthermore, the activity of FadK surged with increasing Mg<sup>2+</sup> concentrations, attaining maximal activity at 0.8 mM Mg<sup>2+</sup>, beyond which no further variations were noted (Fig. 4d). Consequently, we adopted these optimal conditions (pH 7.4, CoA at 0.8 mM, ATP at 0.6 mM and Mg<sup>2+</sup> at 0.8 mM) for subsequent assessments of the activity.

#### 3.4 Thermostability of FadK

To explore how temperature affects activity, we measured activity over a temperature range of 13 to 85 °C. We found that the peak activity at 37 °C, with complete loss of the activity noted at 85 °C (Fig. 5a). Conversely, we evaluated the thermostability of FadK activity at 37 °C, finding that over 90% of the maximum activity persisted following a 2-h incubation at this temperature, and more than 50% of the peak activity of FadK remained intact after 7 h of incubation at 37 °C (Fig. 5b).



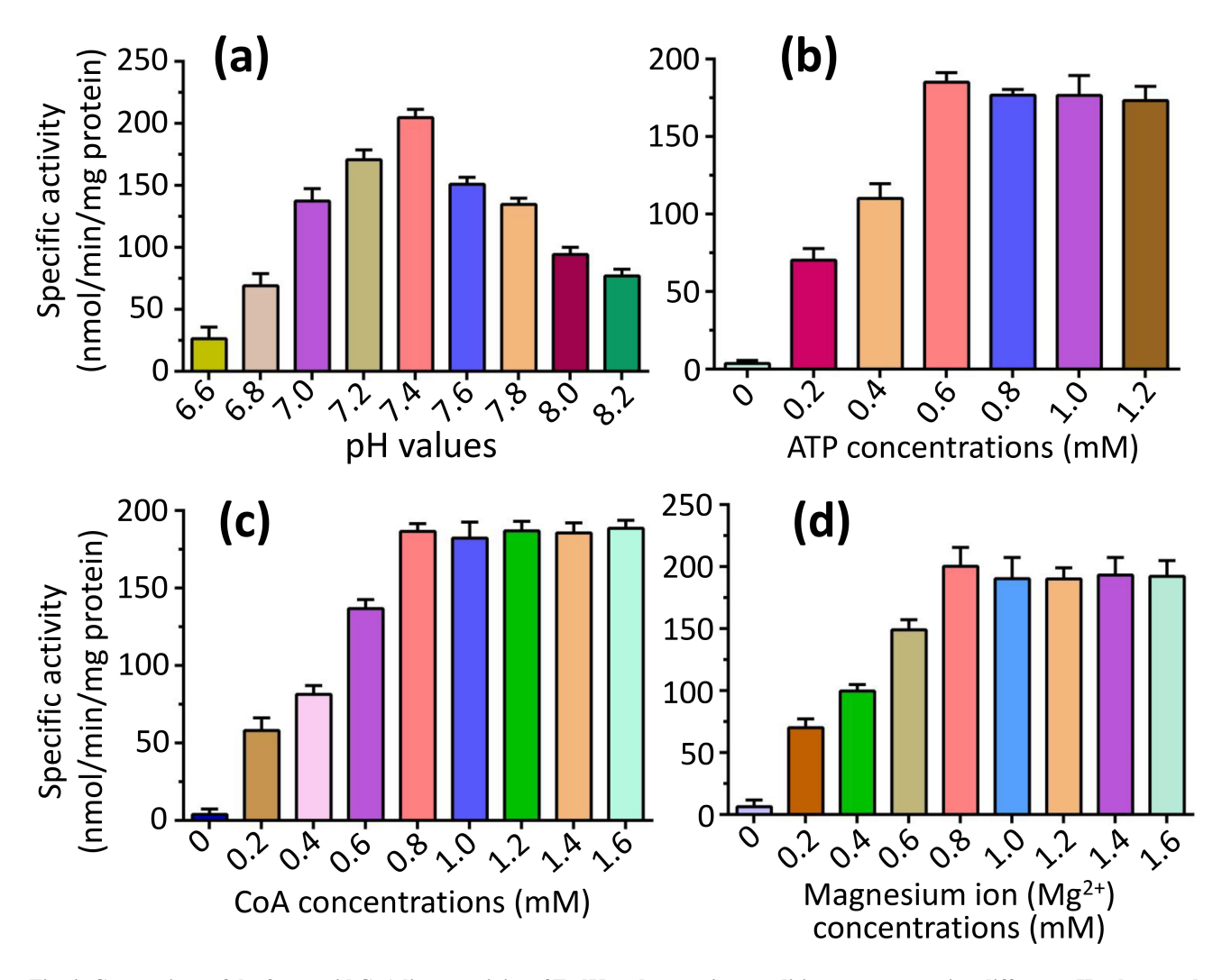


Fig. 4. Comparison of the fatty-acid CoA ligase activity of FadK under varying conditions, encompassing different pH values, and concentrations of ATP, CoA, and  $Mg^{2+}$ . (a) The activity of FadK exhibited an initial increase followed by a decrease with rising pH values, attaining maximal activity at pH 7.4. (b) Increasing concentrations of ATP led to a corresponding increase in activity, peaking at 0.6 mM ATP, beyond which no further change was observed. (c) Similarly, elevating CoA concentrations resulted in heightened activity, reaching a maximum at 0.8 mM CoA, with no subsequent alterations. (d) With increasing  $Mg^{2+}$  concentration, the activity of FadK escalated, achieving maximum activity at 0.8 mM  $Mg^{2+}$ , followed by stability in activity levels.

# 3.5 Kinetic Profile of Protein FadK

We conducted a kinetic analysis of FadK across various concentrations of caprylic acid, hexanoic acid, butyric acid, and capric acid. We observed an increase in the specific activities of FadK with an increase in the substrate concentration, plateauing at 400  $\mu$ M (Fig. 6). The Michaelis constant ( $K_m$ ) for caprylic acid was 330.2  $\mu$ M, notably lower than those of other tested substrates, including butyric acid (946.4  $\mu$ M), hexanoic acid (857.2  $\mu$ M), and capric acid (749.5  $\mu$ M) (**Supplementary Table 2**). This suggested that of the four substrates, FadK showed the highest level of activity on caprylic acid. Among these substrates, caprylic acid was found to be the optimal substrate for FadK (Fig. 6), in agreement with our previous results (Fig. 3).

#### 3.6 Inhibition of the Activity of FadK

The primary aim in identifying and characterizing specific proteins lies in their potential as novel targets for the development of therapeutics. FadK emerges as one such newly discovered candidate. Recent investigations have utilized various nonhydrolyzable acyl-AMP analogs, including dodecyl-AMP, as mechanism-based inhibitors, which have demonstrated potent inhibitory effects on related adenylate-forming enzymes [46]. We examined the inhibitory impact of dodecyl-AMP on FadK activity, and observed a concentration-dependent inhibition, with over 90% reduction in activity at 2  $\mu M$  (Fig. 7a). The half-maximal effective concentration (EC50) of the inhibitor dodecyl-AMP was calculated to be 0.56  $\mu M$ , notably less than 10 times the concentration of FadK employed in the experiments. Furthermore, we investigated whether the



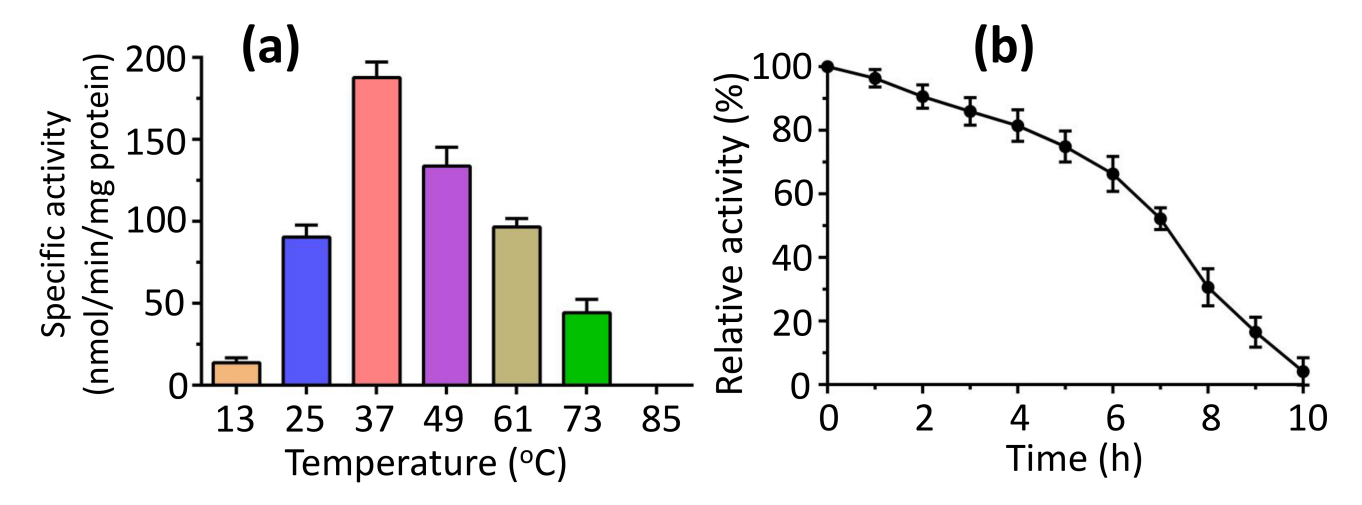


**Fig. 5. Temperature stability of the fatty-acid CoA ligase activity of FadK.** (a) The impact of temperature on FadK activity revealed optimal activity at 37 °C, while FadK demonstrated complete inactivity at 85 °C. (b) Analysis of temperature stability indicated a decline in FadK activity over time.

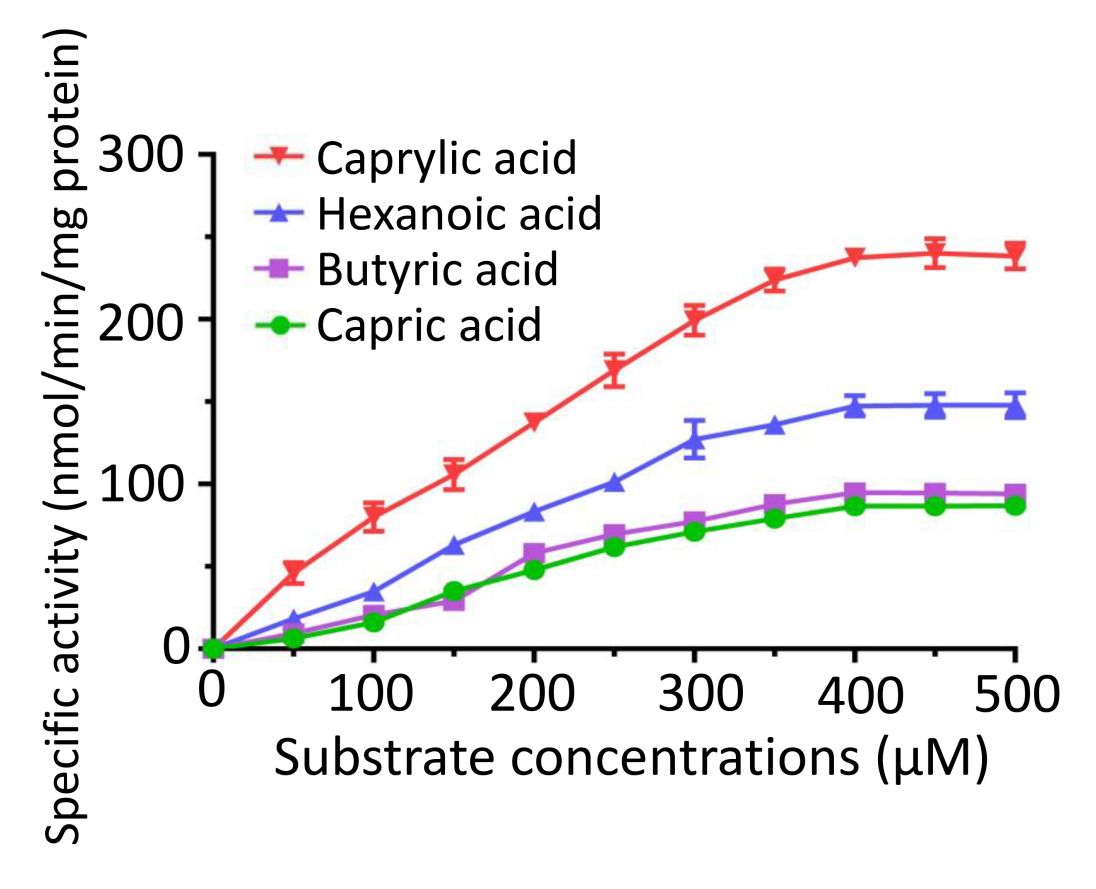


Fig. 6. Enzymatic characterization of FadK across different substrate concentrations. Kinetic profiles were constructed by assessing the activity of FadK using multiple substrates (caprylate, hexanoic acid, butyrate, and capric acid).

inhibitor influenced bacterial growth. We found a dose-dependent inhibition of growth when the inhibitor was added to bacterial suspensions, with almost 90% loss of viability at 65  $\mu M$  (Fig. 7b). These results underscore the impact of dodecyl-AMP inhibitor on the fatty acid CoA metabolism of bacterial strains, thereby influencing bacterial growth.

### 3.7 RT-qPCR Analysis of Gene FadK

The central goal of the identification and functional characterization of essential, distinct proteins in *E. coli* is their potential as therapeutic targets for novel antibacterial agents [47,48]. Among these candidates, FadK has attracted attention as a viable drug target. Non-hydrolyzable acyl-AMP mimetics screened as mechanism-driven in-



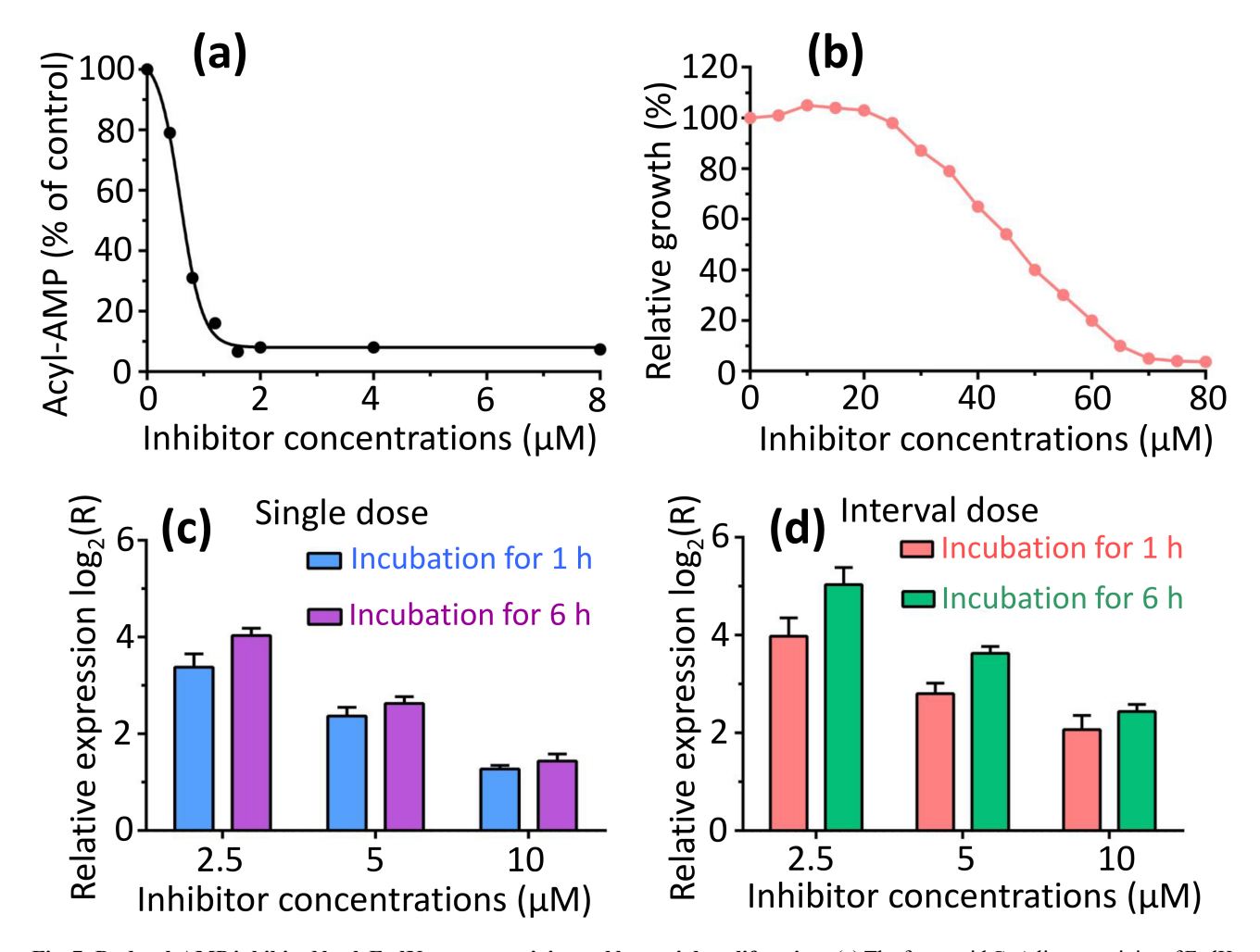


**Fig. 7. Dodecyl-AMP inhibited both FadK enzyme activity and bacterial proliferation.** (a) The fatty-acid CoA ligase activity of FadK was assessed with the increase of dodecyl-AMP concentrations, revealing a decline in activity with increasing inhibitor concentrations. (b) Bacterial growth exhibited progressively stronger inhibition with rising inhibitor concentrations. (c,d) Gene *FadK* levels were measured via real-time quantitative polymerase chain reaction (RT-qPCR). Gene *FadK* expression levels were evaluated under single dose (c) and interval dose (d) conditions.

hibitors show potent inhibition against adenylate forming enzymes such as FadK, highlighting their therapeutic relevance [47–49]. We hypothesized that dodecyl-AMP would serve as a potent inhibitor of the fatty-acid CoA ligase activity of FadK.

To delve into the antibacterial mechanism of the dodecyl-AMP inhibitor at a molecular level, we quantified the expression of the FadK gene via RT-qPCR across a range of inhibitor concentrations. To ensure the viability of  $E.\ coli$  during qPCR signal measurement, we employed two approaches: (1) using the inhibitor at low concentrations (2.5, 5 and 10  $\mu$ M), and (2) involving interval addition of the inhibitor.

We found a dose-dependent up-regulation of the FadK gene with increasing concentrations of the inhibitor (Fig. 7c,d). At singular doses, the FadK gene exhibited up-regulation by 10.2-, 5.3-, and 2.4-fold at 2.5, 5 and 10  $\mu$ M inhibitor after incubation for 1 h, respectively. Similarly, following a 6-h incubation, up-regulation was noted

at 16.2-, 6.2-, and 2.7-fold for the same concentrations (Fig. 7c). With interval dosing, the FadK gene displayed up-regulation by 15.7-, 7.0-, and 4.2-fold at 2.5, 5 and 10  $\mu$ M inhibitor after incubation for 1 h, while after 6 h, up-regulation was observed at 32.7-, 12.4-, and 5.4-fold for the respective concentrations (Fig. 7d). These differential expression profiles of the FadK gene underscore its physiological importance in the fatty acid CoA metabolism for the survival of the bacteria.

# 4. Discussion

In this study, we obtained FadK in monomeric form and identified caprylic acid as its optimal substrate, exhibiting maximum activity at 400  $\mu M$  concentration. The optimal conditions for the fatty-acid CoA ligase activity of FadK were determined as pH 7.4 at 37 °C, with 0.8 mM CoA, 0.6 mM ATP and 0.8 mM Mg²+, respectively. We observed a decrease in FadK activity with increasing concentrations of dodecyl-AMP. Our work elucidates the cat-



alytic behavior of FadK and sheds light on its preference for specific fatty acid substrates, providing critical insights for designing innovative therapies targeting *E. coli* infections.

A previous study has indicated that the expression of the *FadK* gene is suppressed during aerobic growth [29]. *FadK* gene expression reaches its peak under anaerobic conditions when fumarate, the terminal electron acceptor, is present. This enzyme preferentially catalyzes reactions with short-chain fatty acid substrates. In contrast, our study provides a more comprehensive analysis, identifying the optimal conditions for FadK catalytic activity as pH 7.4, 0.6 mM ATP, 0.8 mM CoA, 0.8 mM Mg<sup>2+</sup>, and 37 °C. Caprylic acid was found to be the most effective substrate for FadK activity. Moreover, dodecyl-AMP was shown to inhibit both FadK enzymatic function and bacterial growth. Additionally, we explored the thermostability and kinetic characteristics of FadK with various substrates.

Owing to the failure to generate protein crystals, structural predictions were derived using AlphaFold2. These persisting limitations prompted further exploration of FadK's functional mechanisms. To identify structural homologs, SWISS-MODEL [50–52] was employed (Supplementary Table 4). Comparative analysis revealed that FadK exhibited amino acid sequence identities of 33.59% with sesquiterpene synthases from *Mycolicibacterium smegmatis*, 33.27% with those from *Thermobifida fusca*, 32.69% with *Streptomyces gandocaensis*, 32.35% with *Escherichia coli*, and 32.32% with *Acinetobacter baumannii* (Supplementary Table 4). Collectively, these findings offered critical clues regarding the structural and functional attributes of FadK in *E. coli*.

Overall, *E. coli* FadK, given its classification within the medium-chain fatty acid CoA ligase family, warrants further investigation to elucidate additional functional and mechanistic intricacies.

### 5. Conclusion

In this work, we reported mechanism and function of *E. coli* FadK: (1) FadK was obtained in monomeric form; (2) Caprylate represents the most suitable substrate for FadK regarding the fatty acid CoA activity; (3) Optimal conditions for FadK catalysis are pH 7.4, 0.6 mM ATP, 0.8 mM CoA and 0.8 mM Mg<sup>2+</sup> at 37 °C; (4) The fatty-acid CoA ligase activity of FadK decreased with increasing dodecyl-AMP concentrations, which was further confirmed by the results of RT-qPCR. Our study elucidated the fatty acid-CoA ligase function of FadK and uncovered its distinct substrate specificity toward fatty acids. These insights enabled the design of novel therapeutics effective against severe, including terminal, *E. coli* infections.

# **Availability of Data and Materials**

The data presented in this study are available in this article (and **Supplementary Materials**), and further inquiries can be directed to the corresponding authors.

### **Author Contributions**

Conceptualization, DL; Data curation, DL; Formal analysis, DL; Investigation, DL, AA, LZ and FY; Methodology, DL; Resources, DL; Software, DL; Validation, DL; Writing — original draft, DL; Writing — review & editing, DL. All authors contributed to editorial changes in the manuscript. All authors have read and approved the final version of the manuscript. All authors have participated sufficiently in the work and agreed to be accountable for all aspects of the work.

# **Ethics Approval and Consent to Participate**

Not applicable.

# Acknowledgment

We thank the staff of BL02U1, BL18U1 and BL19U1 beamlines at Shanghai Synchrotron Radiation Facility, Shanghai, People's Republic of China, for help with X-ray data collections.

# Funding

This research received no external funding.

#### Conflict of Interest

The authors declare no conflict of interest.

# **Supplementary Material**

Supplementary material associated with this article can be found, in the online version, at https://doi.org/10.31083/FBL36701.

#### References

- [1] Anderson JD, 4th, Bagamian KH, Muhib F, Amaya MP, Laytner LA, Wierzba T, et al. Burden of enterotoxigenic Escherichia coli and shigella non-fatal diarrhoeal infections in 79 low-income and lower middle-income countries: a modelling analysis. The Lancet. Global Health. 2019; 7: e321–e330. https://doi.org/10.1016/S2214-109X(18)30483-2.
- [2] Qadri F, Akhtar M, Bhuiyan TR, Chowdhury MI, Ahmed T, Rafique TA, et al. Safety and immunogenicity of the oral, inactivated, enterotoxigenic Escherichia coli vaccine ETVAX in Bangladeshi children and infants: a double-blind, randomised, placebo-controlled phase 1/2 trial. The Lancet. Infectious Diseases. 2020; 20: 208–219. https://doi.org/10.1016/ S1473-3099(19)30571-7.
- [3] Pinto Jimenez CE, Keestra S, Tandon P, Cumming O, Pickering AJ, Moodley A, et al. Biosecurity and water, sanitation, and hygiene (WASH) interventions in animal agricultural settings for reducing infection burden, antibiotic use, and antibiotic resistance: a One Health systematic review. The Lancet. Planetary Health. 2023; 7: e418–e434. https://doi.org/10.1016/S2542-5196(23)00049-9.
- [4] Theuretzbacher U, Blasco B, Duffey M, Piddock LJV. Unrealized targets in the discovery of antibiotics for Gram-negative bacterial infections. Nature Reviews. Drug Discovery. 2023; 22: 957–975. https://doi.org/10.1038/s41573-023-00791-6.
- [5] Tenaillon O, Skurnik D, Picard B, Denamur E. The population genetics of commensal Escherichia coli. Nature Reviews. Mi-



- crobiology. 2010; 8: 207–217. https://doi.org/10.1038/nrmicro2298.
- [6] Mayer C, Borges A, Flament-Simon SC, Simões M. Quorum sensing architecture network in Escherichia coli virulence and pathogenesis. FEMS Microbiology Reviews. 2023; 47: fuad031. https://doi.org/10.1093/femsre/fuad031.
- [7] Pitout JDD, Chen L. The Significance of Epidemic Plasmids in the Success of Multidrug-Resistant Drug Pandemic Extraintestinal Pathogenic Escherichia coli. Infectious Diseases and Therapy. 2023; 12: 1029–1041. https://doi.org/10.1007/ s40121-023-00791-4.
- [8] Ardebili A, Izanloo A, Rastegar M. Polymyxin combination therapy for multidrug-resistant, extensively-drug resistant, and difficult-to-treat drug-resistant gram-negative infections: is it superior to polymyxin monotherapy? Expert Review of Antiinfective Therapy. 2023; 21: 387–429. https://doi.org/10.1080/ 14787210.2023.2184346.
- [9] Magalhães C, Lima M, Trieu-Cuot P, Ferreira P. To give or not to give antibiotics is not the only question. The Lancet Infectious Diseases. 2021; 21: e191-e201. https://doi.org/10.1016/ s1473-3099(20)30602-2.
- [10] Walker MM, Roberts JA, Rogers BA, Harris PNA, Sime FB. Current and Emerging Treatment Options for Multidrug Resistant *Escherichia coli* Urosepsis: A Review. Antibiotics (Basel, Switzerland). 2022; 11: 1821. https://doi.org/10.3390/antibiotics11121821
- [11] Cole ST, Brosch R, Parkhill J, Garnier T, Churcher C, Harris D, *et al.* Deciphering thebiologyof Mycobacterium tuberculosis from thecompletegenomesequence. Nature. 1998; 393: 537–544. https://doi.org/10.1038/31159.
- [12] Glickman MS, Cox JS, Jacobs WR, Jr. A novel mycolic acid cyclopropane synthetase is required for cording, persistence, and virulence of Mycobacterium tuberculosis. Molecular Cell. 2000; 5: 717–727. https://doi.org/10.1016/s1097-2765(00)80250-6.
- [13] Duckworth BP, Nelson KM, Aldrich CC. Adenylating enzymes in Mycobacterium tuberculosis as drug targets. Current Topics in Medicinal Chemistry. 2012; 12: 766–796. https://doi.org/10. 2174/156802612799984571.
- [14] Baran M, Grimes KD, Sibbald PA, Fu P, Boshoff HIM, Wilson DJ, *et al.* Development of small-molecule inhibitors of fatty acyl-AMP and fatty acyl-CoA ligases in Mycobacterium tuberculosis. European Journal of Medicinal Chemistry. 2020; 201: 112408. https://doi.org/10.1016/j.ejmech.2020.112408.
- [15] Bo H, Moure UAE, Yang Y, Pan J, Li L, Wang M, et al. My-cobacterium tuberculosis-macrophage interaction: Molecular updates. Frontiers in Cellular and Infection Microbiology. 2023; 13: 1062963. https://doi.org/10.3389/fcimb.2023.1062963.
- [16] Mondal S, Pal B, Sankaranarayanan R. Mechanistic understanding of bacterial FAALs and the role of their homologs in eukaryotes. Proteins. 2025; 93: 26–37. https://doi.org/10.1002/prot.26576.
- [17] van der Sluis R, Erasmus E. Xenobiotic/medium chain fatty acid: CoA ligase - a critical review on its role in fatty acid metabolism and the detoxification of benzoic acid and aspirin. Expert Opinion on Drug Metabolism & Toxicology. 2016; 12: 1169–1179. https://doi.org/10.1080/17425255.2016.1206888.
- [18] Aderem A, Underhill DM. Mechanisms of phagocytosis in macrophages. Annual Review of Immunology. 1999; 17: 593– 623. https://doi.org/10.1146/annurev.immunol.17.1.593.
- [19] Agarwal P, Gordon S, Martinez FO. Foam Cell Macrophages in Tuberculosis. Frontiers in Immunology. 2021; 12: 775326. https://doi.org/10.3389/fimmu.2021.775326.
- [20] Dong Y, Du H, Gao C, Ma T, Feng L. Characterization of two long-chain fatty acid CoA ligases in the Gram-positive bacterium Geobacillus thermodenitrificans NG80-2. Microbiological Research. 2012; 167: 602–607. https://doi.org/10.1016/j.mi cres.2012.05.001.
- [21] Li M, Zhang X, Agrawal A, San KY. Effect of acetate formation

- pathway and long chain fatty acid CoA-ligase on the free fatty acid production in E. coli expressing acy-ACP thioesterase from Ricinus communis. Metabolic Engineering. 2012; 14: 380–387. https://doi.org/10.1016/j.ymben.2012.03.007.
- [22] Sourjik V, Berg HC. Functional interactions between receptors in bacterial chemotaxis. Nature. 2004; 428: 437–441. https://do i.org/10.1038/nature02406.
- [23] Cole ST, Brosch R, Parkhill J, Garnier T, Churcher C, Harris D, et al. Deciphering the biology of Mycobacterium tuberculosis from the complete genome sequence. Nature. 1998; 393: 537–544. https://doi.org/10.1038/31159.
- [24] Wolfe LM, Mahaffey SB, Kruh NA, Dobos KM. Proteomic definition of the cell wall of Mycobacterium tuberculosis. Journal of Proteome Research. 2010; 9: 5816–5826. https://doi.org/10.1021/pr1005873.
- [25] Gaudet P, Livstone MS, Lewis SE, Thomas PD. Phylogenetic-based propagation of functional annotations within the Gene Ontology consortium. Briefings in Bioinformatics. 2011; 12: 449–462. https://doi.org/10.1093/bib/bbr042.
- [26] Gu S, Chen J, Dobos KM, Bradbury EM, Belisle JT, Chen X. Comprehensive proteomic profiling of the membrane constituents of a Mycobacterium tuberculosis strain. Molecular & Cellular Proteomics: MCP. 2003; 2: 1284–1296. https://doi.org/10.1074/mcp.M300060-MCP200.
- [27] Kelkar DS, Kumar D, Kumar P, Balakrishnan L, Muthusamy B, Yadav AK, et al. Proteogenomic analysis of Mycobacterium tuberculosis by high resolution mass spectrometry. Molecular & Cellular Proteomics: MCP. 2011; 10: M111.011627. https://doi.org/10.1074/mcp.M111.011445.
- [28] Mawuenyega KG, Forst CV, Dobos KM, Belisle JT, Chen J, Bradbury EM, et al. Mycobacterium tuberculosis functional network analysis by global subcellular protein profiling. Molecular Biology of the Cell. 2005; 16: 396–404. https://doi.org/10.1091/ mbc.e04-04-0329.
- [29] Morgan-Kiss RM, Cronan JE. The Escherichia coli fadK (ydiD) gene encodes an anerobically regulated short chain acyl-CoA synthetase. The Journal of Biological Chemistry. 2004; 279: 37324–37333. https://doi.org/10.1074/jbc.M405233200.
- [30] Liu D, Tian Z, Tusong K, Mamat H, Luo Y. Expression, purification and characterization of CTP synthase PyrG in Staphylococcusaureus. Protein Expression and Purification. 2024; 221: 106520. https://doi.org/10.1016/j.pep.2024.106520.
- [31] Liu D, Yuan C, Guo C, Huang M, Lin D. Recombinant expression and functional characterization of FadD2 protein in Mycobacterium tuberculosis. Protein Expression and Purification. 2024; 214: 106377. https://doi.org/10.1016/j.pep.2023.106377.
- [32] Dagsuyu E, Yanardag R. Purification of thioredoxin reductase from Spirulina platensis by affinity chromatography and investigation of kinetic properties. Protein Expression and Purification. 2024; 216: 106417. https://doi.org/10.1016/j.pep.2023.106417.
- [33] Qin H, Guo C, Chen B, Huang H, Tian Y, Zhong L. The C-terminal selenenylsulfide of extracellular/non-reduced thioredoxin reductase endows this protein with selectivity to small-molecule electrophilic reagents under oxidative conditions. Frontiers in Molecular Biosciences. 2024; 11: 1274850. https://doi.org/10.3389/fmolb.2024.1274850.
- [34] Livak KJ, Schmittgen TD. Analysis of relative gene expression data using real-time quantitative PCR and the 2(-Delta Delta C(T)) Method. Methods (San Diego, Calif.). 2001; 25: 402–408. https://doi.org/10.1006/meth.2001.1262.
- [35] Schmittgen TD, Livak KJ. Analyzing real-time PCR data by the comparative C(T) method. Nature Protocols. 2008; 3: 1101– 1108. https://doi.org/10.1038/nprot.2008.73.
- [36] Liu D, Deng H, Song H. Insights into the functional mechanisms of the sesquiterpene synthase GEAS and GERDS in lavender. International Journal of Biological Macromolecules. 2025; 299: 140195. https://doi.org/10.1016/j.ijbiomac.2025.140195.



- [37] Liu D, Song H, Deng H, Abdiriyim A, Zhang L, Jiao Z, et al. Insights into the functional mechanisms of three terpene synthases from Lavandula angustifolia (Lavender). Frontiers in Plant Science. 2024; 15: 1497345. https://doi.org/10.3389/fpls.2024.1497345.
- [38] Liu D, Abdiriyim A, Zhang L, Ruzitohti B. Functional and mechanistic insights into the stealth protein full-length CpsY is conducive to understanding immune evasion mechanisms by Mycobacterium tuberculosis. Tuberculosis (Edinburgh, Scotland). 2025; 152: 102616. https://doi.org/10.1016/j.tube.2025. 102616
- [39] Kuznetsova NA, Kaliya OL. Oxidative photobleaching of phthalocyanines in solution. Journal of Porphyrins and Phthalocyanines. 2012; 16: 705–712. https://doi.org/10.1142/ s1088424612300042.
- [40] Adikesavan AK, Katsonis P, Marciano DC, Lua R, Herman C, Lichtarge O. Separation of recombination and SOS response in Escherichia coli RecA suggests LexA interaction sites. PLoS Genetics. 2011; 7: e1002244. https://doi.org/10.1371/journal.pg en.1002244.
- [41] Ye R, Xu H, Wan C, Peng S, Wang L, Xu H, *et al.* Antibacterial activity and mechanism of action of ε-poly-L-lysine. Biochemical and Biophysical Research Communications. 2013; 439: 148–153. https://doi.org/10.1016/j.bbrc.2013.08.001.
- [42] Rocha DJP, Santos CS, Pacheco LGC. Bacterial reference genes for gene expression studies by RT-qPCR: survey and analysis. Antonie Van Leeuwenhoek. 2015; 108: 685–693. https://doi.or g/10.1007/s10482-015-0524-1.
- [43] Guo F, Ortega-Pierres G, Argüello-García R, Zhang H, Zhu G. Giardia fatty acyl-CoA synthetases as potential drug targets. Frontiers in Microbiology. 2015; 6: 753. https://doi.org/10.3389/fmicb.2015.00753.
- [44] Rosen BC, Dillon NA, Peterson ND, Minato Y, Baughn AD. Long-Chain Fatty Acyl Coenzyme A Ligase FadD2 Mediates Intrinsic Pyrazinamide Resistance in Mycobacterium tuberculosis. Antimicrobial Agents and Chemotherapy. 2017; 61: e02130– 16. https://doi.org/10.1128/AAC.02130-16.

- [45] Kang Y, Zarzycki-Siek J, Walton CB, Norris MH, Hoang TT. Multiple FadD acyl-CoA synthetases contribute to differential fatty acid degradation and virulence in Pseudomonas aeruginosa. PloS One. 2010; 5: e13557. https://doi.org/10.1371/jour nal.pone.0013557.
- [46] Arora P, Goyal A, Natarajan VT, Rajakumara E, Verma P, Gupta R, et al. Mechanistic and functional insights into fatty acid activation in Mycobacterium tuberculosis. Nature Chemical Biology. 2009; 5: 166–173. https://doi.org/10.1038/nchembio.143.
- [47] Ferreras JA, Ryu JS, Di Lello F, Tan DS, Quadri LEN. Small-molecule inhibition of siderophore biosynthesis in Mycobacterium tuberculosis and Yersinia pestis. Nature Chemical Biology. 2005; 1: 29–32. https://doi.org/10.1038/nchembio706.
- [48] Portevin D, de Sousa-D'Auria C, Montrozier H, Houssin C, Stella A, Lanéelle MA, et al. The acyl-AMP ligase FadD32 and AccD4-containing acyl-CoA carboxylase are required for the synthesis of mycolic acids and essential for mycobacterial growth: identification of the carboxylation product and determination of the acyl-CoA carboxylase components. The Journal of Biological Chemistry. 2005; 280: 8862–8874. https://doi.org/10.1074/jbc.M408578200.
- [49] Léger M, Gavalda S, Guillet V, van der Rest B, Slama N, Montrozier H, et al. The dual function of the Mycobacterium tuberculosis FadD32 required for mycolic acid biosynthesis. Chemistry & Biology. 2009; 16: 510–519. https://doi.org/10.1016/j.chembiol.2009.03.012.
- [50] Bertoni M, Kiefer F, Biasini M, Bordoli L, Schwede T. Modeling protein quaternary structure of homo- and hetero-oligomers beyond binary interactions by homology. Scientific Reports. 2017; 7: 10480. https://doi.org/10.1038/s41598-017-09654-8.
- [51] Bienert S, Waterhouse A, de Beer TAP, Tauriello G, Studer G, Bordoli L, et al. The SWISS-MODEL Repository-new features and functionality. Nucleic Acids Research. 2017; 45: D313– D319. https://doi.org/10.1093/nar/gkw1132.
- [52] Waterhouse A, Bertoni M, Bienert S, Studer G, Tauriello G, Gumienny R, et al. SWISS-MODEL: homology modelling of protein structures and complexes. Nucleic Acids Research. 2018; 46: W296–W303. https://doi.org/10.1093/nar/gky427.

